Chaotic Modeling and Simulation (CMSIM) **1: 59-79, 2019**

Chaos in Complex and Quaternion Blaschke Maps

David C. Ni

Direxion Technology
9F, No. 177-1, Ho-Ping East Road, Daan District, Taipei, 106, Taiwan, ROC

Abstract. We have explored chaotic phenomena of extended Blaschke products, which are the generalized form of nonlinear Lorentz transformation, in conjunction with triplet momentum space (linear-angular-spin momentum) on the complex plane for simulation of N-body systems in the context of dynamical systems. The results demonstrate that our construction has built-in structures for modelling several challenging phenomena, such as Dark Matters, Dark Energy, formation of Stellar Systems, Quantum Uncertainty, Phase and Superconductor Transitions etc., particularly when the structures evolving from stable forms to chaos, where we have observed formation of hierarchical systems.
In this work, we further extend the effort from complex mapping to quaternion mapping for simulating the related chaotic phenomena as well as for unifying standard model of elementary particles into this framework. Finally, we correlate complex mapping with quaternion mapping.
Keywords: Complex, Quaternion, Blaschke, Triplet momentum space

1 Introduction

Contemporary models for N-body systems are mainly extended from temporal, two-body, and mass point representation of Newtonian mechanics. Other mainstream models include 2D/3D Ising models constructed from the lattice structures. These models have been adopted for simulations in different branches of physics, nevertheless, have also encountered challenges in the new observations such as dark matter and dark energy. We were therefore motivated to develop a new construction directly from complex-variable N-body systems based on the extended Blaschke functions (EBF)[1], which represent a non-temporal and nonlinear extension of Lorentz transformation on the complex plane – the normalized linear-angular-spin space. A point on the complex plane represents a normalized state of linear, angular and spin momentum observed from a reference frame in the context of the theory of special relativity. This nonlinear representation couples linear, angular, and spin momentum in conjunction with nonlinearity of EBF.

The convergent sets in domain and corresponding codomain demonstrated hierarchical structures and topological transitions depending on parameter space. Among the transitions, continuum-to-discreteness transitions, nonlinear-to-linear transitions, and phase transitions manifest this construction embedded with structural richness for modelling broad categories of physical phenomena.

Received: 9 July 2018 / Accepted: 12 December 2018

ISSN 2241-0503

In addition, we have recently developed a set of new algorithms for solving EBF iteratively in the context of dynamical systems. The mapped sets generally follow the Fundamental Theorem of Algebra (FTA), however, exceptional cases are also identified. The mapped sets show a form of $\sigma + i\,[-t, t]$, where σ and t are the real numbers, and the $[-t, t]$ shows canonical distributions. The hierarchical structures in domain are proposed to model the family of elementary particles. Based on this connection, the hierarchical layers may be 1, 3, and 5 depending on the normalized linear momentum. The 5-layer case is adopted for interpreting dark matter.

As in the previous papers [2,3,4,5,6,7], we introduce a spin momentum to the EBF, and for the degree of EBF, n, is greater than 2, we observed that the fractal patterns showing lags as shown in Fig. 10(a). As angular momentum increases, the divergent sets (fractal patterns) are connected to the adjacent sets and diffuse as shown in Fig. 10(a). As iteration further increasing, subsequently all convergent sets will become null set. The main effort is to extend the mapping algorithm to the transition regions, where the sets in domains and codomains becoming chaotic state. Particularly, we characterize the convergent sets in codomain near the chaotic transition. As an example of efforts on the applications of modeling the physical phenomena, we apply the observations to the theories of formation of galaxy clusters and stellar systems. The different stable sets are adopted for interpreting dark energy.

On complex plane, however, spin momentum is limited to a single and discrete value for performing functional mapping, therefore, we extend to quaternion maps for further exploring the chaotic transitions as well as for potentially modelling Standard model of elementary particles with set structures forming group representations [8 and ref. therein], which are the framework of quantum formalism for theorizing family structure of elementary particles. We then consistently correlate quaternion mapping with complex mapping in domains and codomains.

2. Construction

2.1 Functions and Equations

Given two inertial frames with different momentums, u and v, the observed momentum, u', from v-frame is as follows:

$$u' = (u - v) / (1 - vu/c^2) \tag{1}$$

We set $c^2 = 1$ and then multiply a phase connection, $exp(i\psi(u))$, to the normalized complex form of the equation (1) to obtain the following:

$$(u'/u) = exp(i\psi(u))(1/u)[(u-v)/(1-uv)] \tag{2}$$

We hereby define a generalized complex function as follows:

$$f_{B,}(z,m)= z^{-1}\, \Pi^m C_i \qquad (3)$$

And C_i has the following forms:

$$C_i = exp(g_i(z))[(a_i\text{-}z)/(1\text{-}\bar{a}_i z)] \qquad (4)$$

Where z is a complex variable representing the momentum u, a_i is a parameter representing momentum v, $\bar{a}_i$ is the complex conjugate of a complex number a_i and m is an integer. The term $g_i(z)$ is a complex function assigned to $\Sigma^p 2p\pi iz$ with p as an integer. The degree of $f_B(z,m) = P(z)/Q(z)$ is defined as Max{deg P, deg Q}. The function f_B is called an extended Blaschke function (EBF). The extended Blaschke equation (EBE) is defined as follows:

$$f_B(z,m) - z = 0 \qquad (5)$$

2.2 Domain and Codomain

A domain can be the entire complex plane, C_∞, or a set of complex numbers, such as $z = x+yi$, with $(x^2 + y^2)^{1/2} \leqq R$, and R is a real number. For solving the EBF and EBE, a function f will be iterated as:

$$f^{\,n}(z) = f \circ f^{\,n-1}(z), \qquad (6)$$

Where n is a positive integer indicating the number of iteration. The function operates on a domain, called domain. The set of $f^{\,n}(z)$ is called mapped codomain or simply a codomain. In the figures, the regions in black color represent stable Fatou sets containing the convergent sets of the concerned equations and the white (i.e., blank) regions correspond to Julia sets containing the divergent sets, the complementary sets of Fatou sets on C_∞ in the context of dynamical systems.

2.3 Parameter Space

In order to characterize domains and codomains, we define a set of parameters called parameter space. The parameter space includes six parameters: 1) z, 2) a, 3) *exp(gi(z))*, 4) m, 5) *iteration*, and 6) *degree*. In the context of this paper we use the set {z, a, *exp(gi(z))*, m, *iteration*, *degree*} to represent this parameter space. For example, {a}, is one of the subsets of the parameter space.

2.4 Domain-Codomain Mapping

On the complex plane, the convergent sets in domains of the EBFs form fractal patterns of the limited-layered structures (i.e., Herman rings), which demonstrate skip-symmetry, symmetry broken, chaos, and degeneracy in conjunction with parameter space [7]. Fig. 1 shows a circle in the domain is mapped to a set of twisted figures in the codomain. We deduce that the mapping related to the tori structures in conjunction with EBFs. Fig. 2 shows two types of fractal patterns in the domains. These patterns are plots at different scales. In order to demonstrate these figures, we reverse the color tone of Fatou and Julia sets, namely, the black areas are the divergent sets.

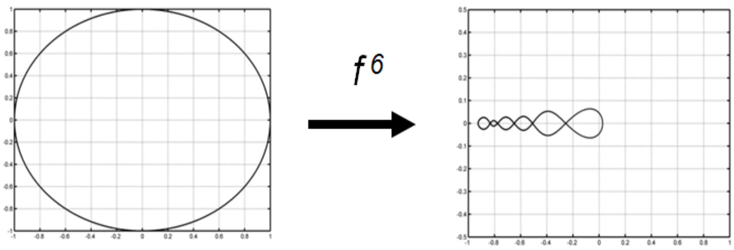

Fig. 1. Domain-Codomain mapping of a unit circle.

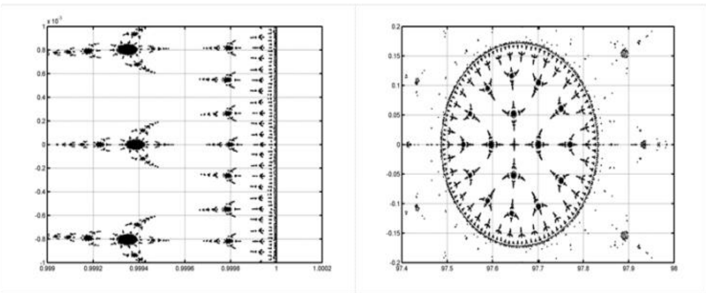

Fig. 2. Fractal Patterns of the divergent sets in domains.

2.5 Convergence and Divergence of Iterated Sequence

The convergence and divergence of a given point on the complex plane are further examined by plotting the iterated sequence of absolute values of EBFs. Fig. 3(a) shows a case of divergence with *iteration = 100*. Fig. 3(b), 3(c), and 3(d) show convergent sequences. More rigorous definitions of convergence and divergence in conjunction with programming algorithms are part of the forward efforts of this effort.

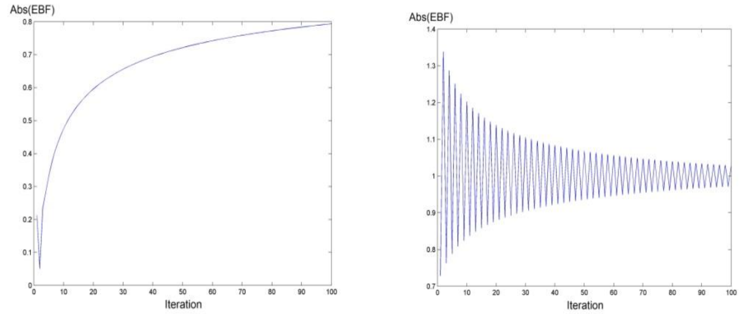

(a) Divergent sequence (b) Convergent sequence

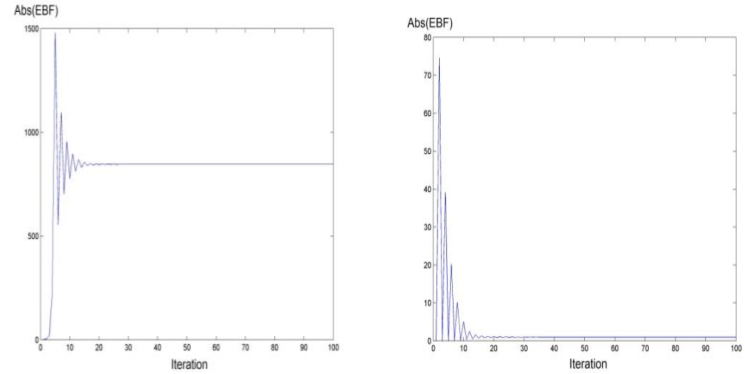

(c) Convergent sequence (d) Convergent sequence

Fig. 3. Divergence and Convergence of iterated sequence of EBF

3. Transitions

3.1 Nonlinear to Linear Transitions

Fig. 4 shows the convergent sets of domains with different degrees and values of parameter $\{a\}$. Fig. 4 (a) through (d) show that the convergent sets are quite topologically different for different degrees, from $f_B(z,1)$, the linear equation to $f_B(z,4)$. When the value of $\{a\}$ increases from 0.1 to 0.8.

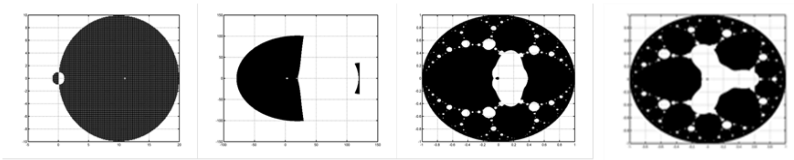

(a) $f_B(z,1)$, $a=0.1$ (b) $f_B(z,2)$, $a=0.1$ (c) $f_B(z,3)$, $a=0.1$ (d) $f_B(z,4)$, $a = 0.1$

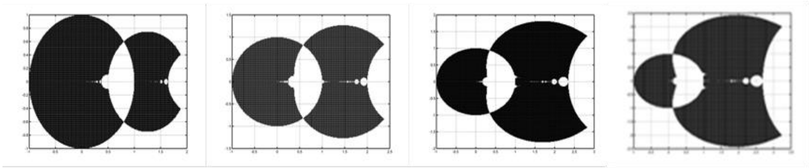

(e) $f_B(z,1)$, $a=0.8$ (f) $f_B(z,2$, $a=0.8$ (g) $f_B(z,3)$, $a=0.8$ (h) $f_B(z,4)$, $a = 0.8$

Fig. 4. Convergent sets of $f_B(z,1)$, $f_B(z,1)$, $f_B(z,1)$, and $f_B(z,1)$ with values of $\{a\}$ at *0.1* and *0.8* respectively. The convergent sets show topologically similar with minor variations as shown from $f_B(z,1)$, the linear equation to $f_B(z,4)$ or even at higher degrees as in Fig. 4 (e) through (h). We call this phenomenon as nonlinear-to-linear transition.

3.2 Continuum to Discrete Transitions

When the value of $\{a\}$ approaches to unity, the topological patterns of convergent sets in domains demonstrate an abrupt or quantum-type transition from the connected sets to the discrete sets. The discrete sets show Cantor-like pattern when mapping onto real axes on the complex plane, nevertheless, these sets are not Cantor sets by definition [6, 7, 9, 10].

The transition of EBF occurs between $a = 1 – 10^{-16}$ and $a = 1 – 10^{-17}$. Fig. 5 shows this type of topological transition. Fig. 5(a) through 5(d) shows the nonlinear-to-linear degeneracy, and 4(e) shows the Cantor-like pattern at all degrees once the transition occurs. Here, we define $\Delta = 1 - a$. Fig. 6 shows another discreteness-to-continuum transition around a pole in original domains based on the parameter $\{degree\}$. Fig. 7 shows continuum-to-discreteness transitions in codomain based on the parameter $\{iteration\}$. These transitions demonstrate a fabric tori structure of EBFs.

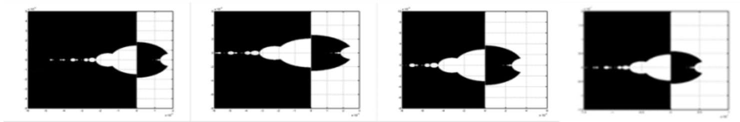

(a) $f_B(z,1)$ *(b)* $f_B(z,2)$ *(c)* $f_B(z,3)$ *(d)* $f_B(z,10)$
All with $\Delta \sim 10^{-16}$

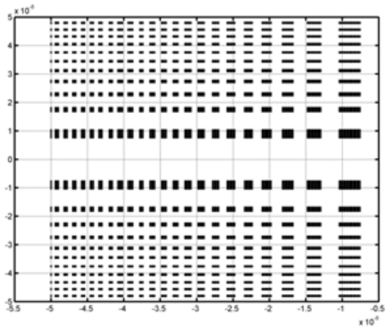

(e) $f_B(z,m), \Delta = 10^{-17}$

Fig. 5. Connected sets transit to discrete Cantor-like sets for all $f_B(z,m)$ *At* $\Delta = 10^{-17}$ in domains.

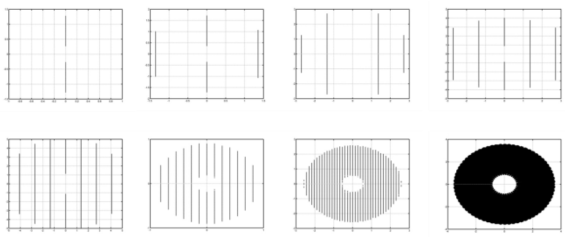

Fig. 6. Discreteness to continuum transitions around a pole of EBF as value {*degree*} increases in domains.

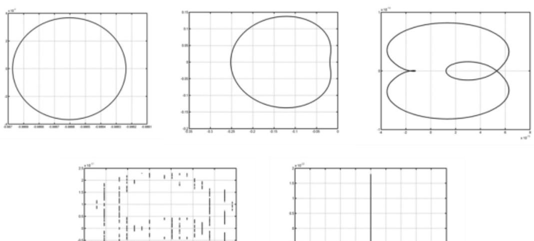

Fig. 7. Continuum to discreteness transitions as value {*iteration*} increases in domains.

3.3 Topological Transitions

Fig. 8 shows a mapping from the convergent sets of domain to codomain. This is a point-to-point mapping at same position between domain and codomain. We examine the plots of three different values: absolute, real, and imaginary on the complex plane. The plots of absolute and real values show a modular pattern with 90 degree rotation. These sets are symmetrical to the y-axis, comparing to the x-axis symmetry of the convergent sets of the domain. The plots of imaginary values demonstrate conjugate symmetry to the y-axis. Fig. 9 further shows this special feature with different values of $\{a\}$. Using the color bar (with $z = 0$ at center of the bar) on the right side of individual figures in Fig. 9, we observe the relationship of $z(-x, y) = -z(x, y)$, and define as conjugate symmetry.

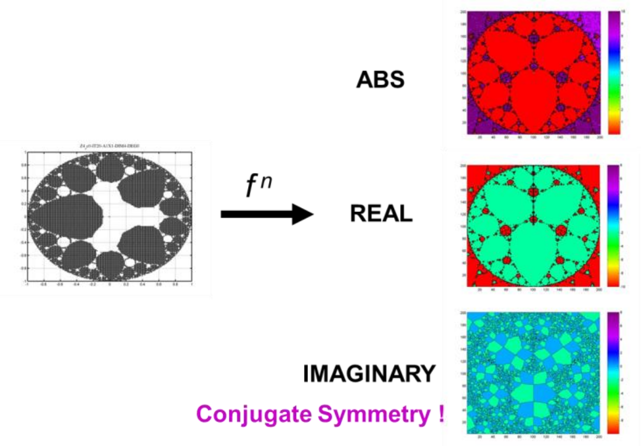

Fig. 8. Separation of Real and Imaginary values in Domains

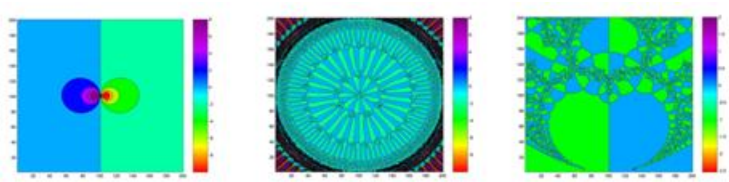

Fig. 9. Three patterns of conjugate symmetry at different values of $\{a\}$.

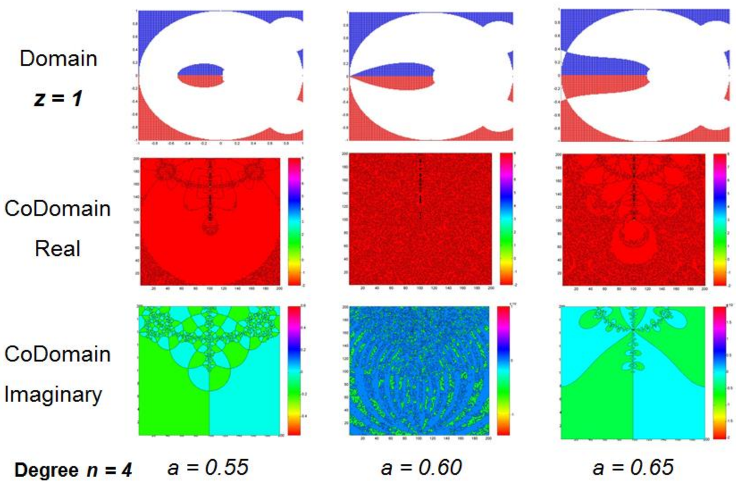

Fig. 10 Topological Transitions in Domain and CoDomain

Fig. 10 shows topological transitions as value of $\{a\}$ increases from *0.55* to *0.65*. The transition value (i.e., $a = 0.60$ in Fig. 10) depends on the *degree* (n) that as degree increases, the transition value increases. Among the transitions, we also observe that the imaginary values transfer from complementary symmetry to a single value as value of $\{a\}$ approaches to *0*. Fig. 11 shows these transitions as $a = 10^{-105}$ decreases to $a = 10^{-108}$.

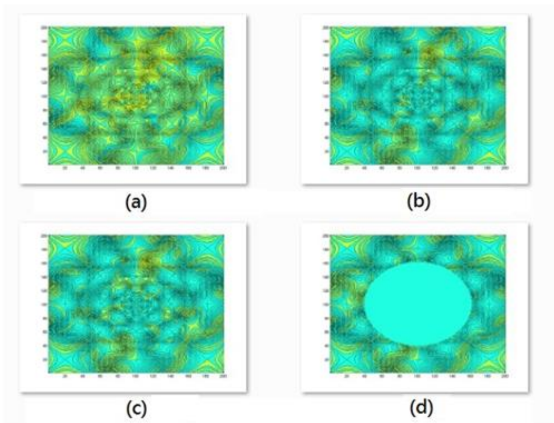

(a) $a = 10^{-105}$ (b) $a = 10^{-106}$ (c) $a = 10^{-107}$ (d) $a = 10^{-108}$

Fig. 11 Superconductor Transitions

3.4 Chaotic Transitions

The convergent sets are colored in blue for those on the upper half of the complex plane, while those sets in red color are on the lower half intendedly as in Fig. 10. By doing so, we are able to examine the mappings in more details.

When an additional spin momentum applied to EBF as equation 7 below:

$$a = 0.1(\cos\theta + \sin\theta) \quad \text{with } degree = 4 \tag{7}$$

In Fig. 12(a), each layer or level of fractals, namely, the divergent sets in domain will be lagged more as the value θ increases, and subsequently connected to the adjacent divergent sets, and eventually the divergent areas will enlarging diffuse and become null sets for value of {*degree*} is greater than 2 as shown in Fig. 12(a). For value of {*degree*} is *1* or *2*, as shown in Fig. 12(b), this type of diffusion will not occur as shown in Fig. 12(b) [3, 4].

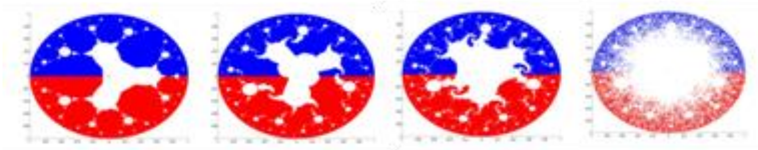

(a) *degree = 4*

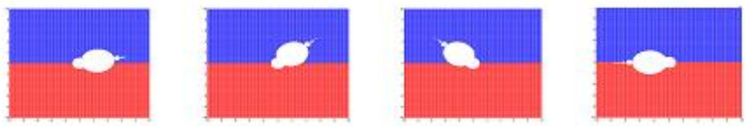

(b) *degree = 1 or 2*

Fig. 12. Transitions of convergent sets in domain as spin increases

4. Mapped Sets of Linear-Angular Momentum

4.1 Mapped sets in Domain and Codomain

As shown in Fig. 13, a set of algorithms are developed for mapping EBFs, and the discrete sets in codomain demonstrate fixed-point-like mapped sets. The upper half and lower half plane are colored in blue and red individually for the purpose examining domain-codomain mapping. This type of mapping is value mapping that the mapped complex values are directly plotted on the codomain.

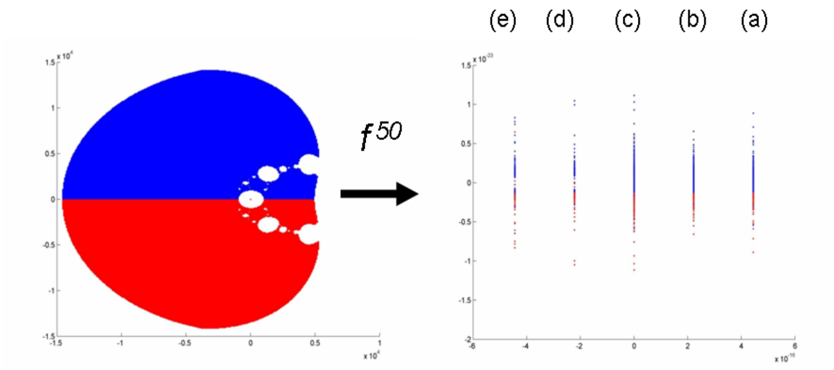

(a) Domain (b) Codomain

Fig. 13. Value mapping from convergent sets of domain to codomain

Fig. 13. shows the iterated sets of EBF for $a = 0.1$ and *degree* $= 3$ at scale of 10^4 as convergent set on the domain (13(a)) mapped to the convergent set (a), (b), (c), (d) and (e) on the codomain (13(b)) violating Fundamental Theorem of Algebra (FTA), which asserts that the number of mapped sets is equal to the degree of EBF.

For the individual convergent sets shown in Fig. 13 (b) in codomain, we can examine closely which sets or subset in domain are mapped from as shown in Fig. 14. These figures demonstrate a deterministic perspective against the uncertainty of mapping and may fundamentally change the definition of probability in the context of statistics.

(b)

(e)

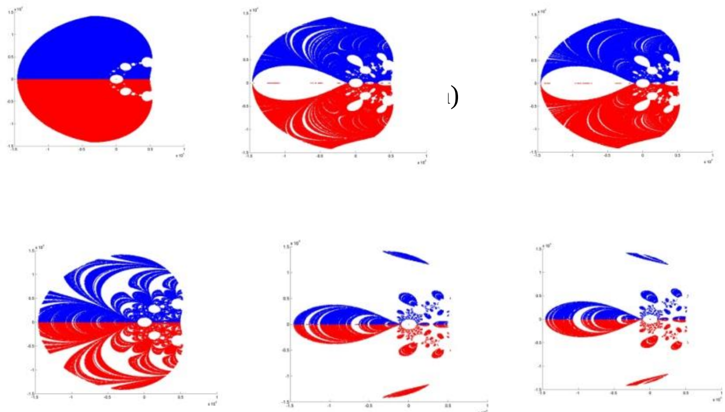

Fig. 14. The individual sets in domain (13(a)) corresponding to the convergent set (a), (b), (c), (d) and (e) in codomain (13(b)).

Fig. 15 shows mapped sets for EBFs with *degree=7* and *degree=12* individually, which are asserted by FTA. The mapped sets show that the individual sets with specific real values are with spread-out imaginary sets demonstrating various distributions.

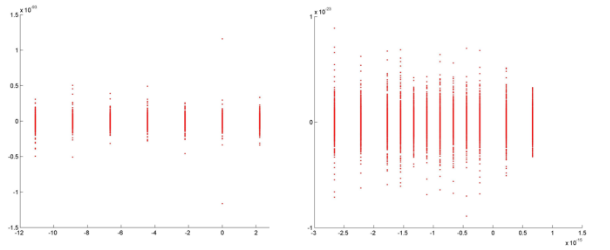

(a) $f_B(z,7)$ *(b)* $f_B(z,12)$)

Fig. 15. Two mapped sets with two different values of {*degree*}.

For *degree=1*, the mapped sets shows transition from *1* mapped set to *2* mapped sets as value of {*a*}increases from *0.68* to *0.69*. This observation is proposed to model the phenomenon of symmetry broken.

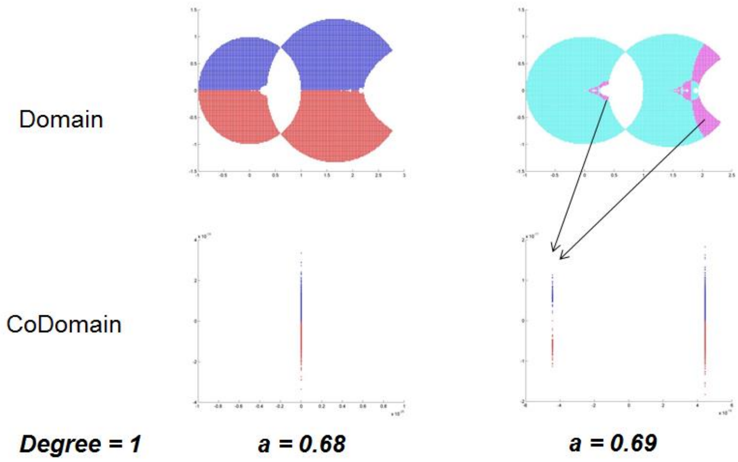

Fig. 16. Mapped sets of *degree* = *1* show transition and violation of FTA

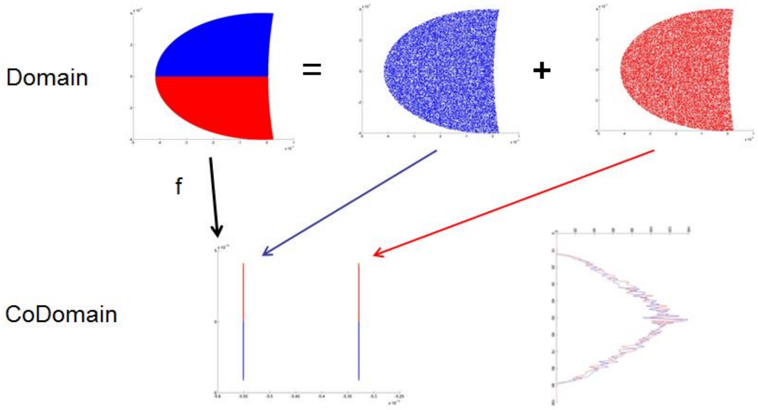

Fig. 17. Mapped sets of *degree* = *2* show uncertainty in domain

For *degree=2*, the mapped sets show random sets of mapping sets in domain to 2 sets in codomain as shown in Fig. 17. The distributions of the mapped sets are shown at right-bottom of Fig. 17 and are proposed to model uncertainty in quantum formalism.

4.2 Distributions

For the individual convergent sets shown in Fig. 13 (b), we further plot the distributions of real and imaginary sets with a designated partition as shown in Fig. 18. The real distributions show the distribution of linear momentum, while the imaginary distribution shows overall distribution of the angular momentum [10, 11].

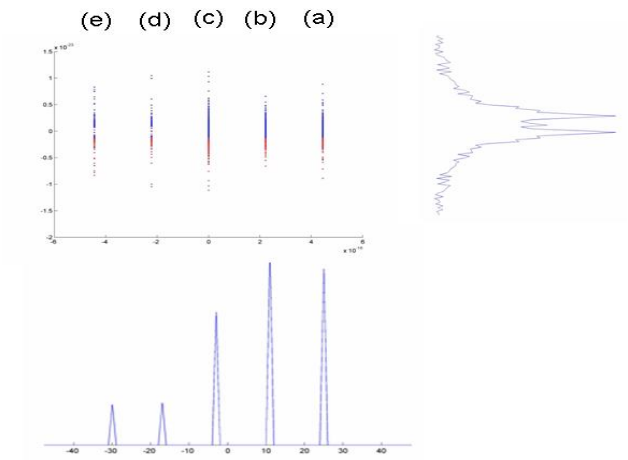

Fig. 18. Distribution plots of convergent sets in the codomain as in Fig. 13(b).

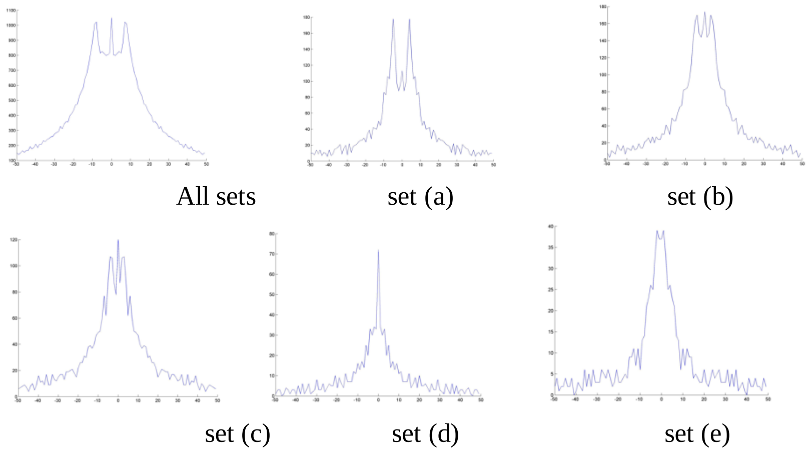

Fig. 19. Distribution plots of individual convergent sets in the codomain.

Further, we plot the distributions of the all and individual sets in Fig. 13 and Fig. 14 as shown in Fig. 19. These distributions demonstrate 1-peak, 2-peak, and 3-peak distributions with different peak values. The patterns of these distributions demonstrate scaling invariant to the parameter {*iteration*}.

4.3 Hierarchical Structures

Depending on value of linear momentum, {*a*}, we observe 5 layers of hierarchical concentric rings as shown in Fig. 20. The regions in black are the convergent regions, which show fractal patterns particularly as Fig. 20(c), the unit disc with fractal divergent regions.

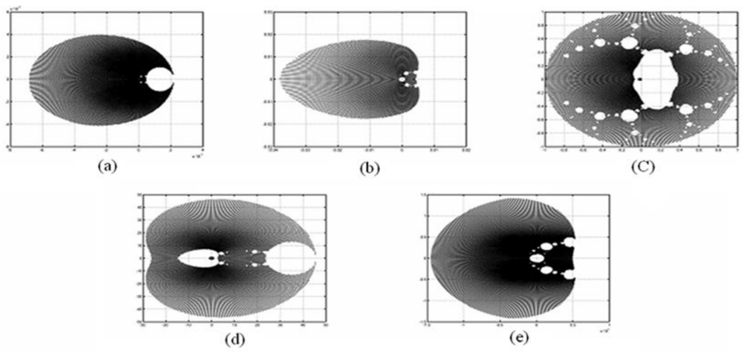

Momentum-dependent scales (a) 10^{-6} (b) 10^{-2} (c) Unit Disc (d) 10^{2} (e) 10^{6}. All ring structures are around *z = 0.*

Fig. 20. Distribution plots of individual convergent sets in the codomain.

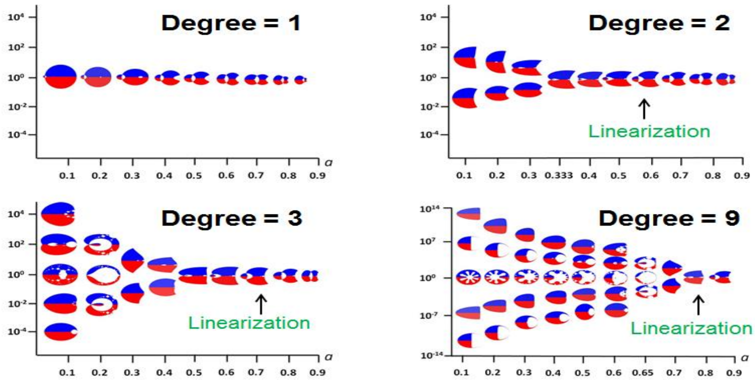

Fig. 21. Hierarchical structures with nonlinear degree = 1, 2, 3, and 9 and the dependencies on linear momentum as well as functional degree.

Fig. 21 shows the dependency of convergent sets on linear momentum and degree. For *degree = 1*, we observe only one ring for all normalized linear momentum is less than 1. For *degree = 2*, we observe two-layer hierarchy when the normalized linear momentum is less than about *0.333*, where the nonlinear to linear transition occurs. For degree is equal or greater than three, we observe 5-layer hierarchy transits to 3-layer hierarchy, then to 2-layer hierarchy, and finally to one-layer hierarchy accordingly. In the transition zones, the related layers are connected and merged. In addition, the patterns (referred to Fig. 10) will be randomized in the transition zones. We propose that the 5-layer structures with dependency for modelling so-called dark matters, namely, currently existing 3 hierarchical elementary families will be extended to 5 hierarchical families. The hidden families with momentum dependency are the dark matters.

5. Mapped Sets of Linear-Angular-Spin Momentum

Applying the methods described in the section 4 to the convergent sets in chaotic transitions described in section 3.4, we can examine closely the convergent sets in both domains and codomains.

5.1. Mapped sets in Domain and Codomain

As described in equation (7) in section 3.4., we have the following parameters as in equation (8):

$$a = 0.2\,(\cos(75*\pi/180) + \sin(75*\pi/180)) \quad \text{with } degree = 3 \quad (8)$$

As the value θ increases and the convergent sets approaching to the chaotic transitions, two divergent sets are both diffusing to the sub-fractal sets and demonstrate a balanced diffusion. Subsequently, the sets converge slowly and present a hierarchical structure of several layers, which are viable for the modelling of observed phenomena such as dark energy. Fig. 22 shows the plots the distributions of the convergent sets in the codomain of equation (8).

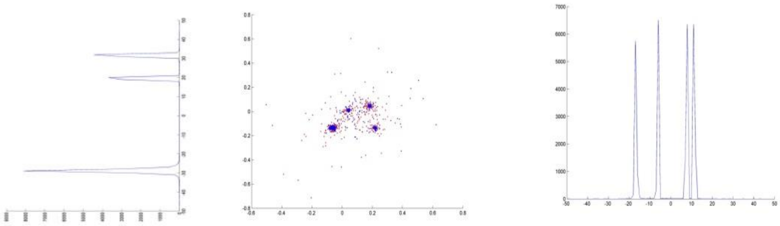

Fig. 22. The distributions of convergent sets for *a = 0.2*, *θ=(75*π/180)* and *degree = 3* in the codomain.

Further examining the distributions of the convergent sets, both distributions of the real and imaginary values are not symmetrical. Comparing the plots in Fig. 23 against those in Fig. 19 (spin momentum set to null), we observe symmetry broken when spin momentum is introduced into domain-codomain mapping.

The important ideas from these plots for the theoretical constructions are that in the chaotic transitions, the values of momentum and angular momentum are in limited discrete groups. This observation manifests that we can model the turbulence, chaos, and related phenomena more straightforward in linear-angular-spin momentum space than those in temporal space. In the following section, we will further extend this construction based on hierarchical structures.

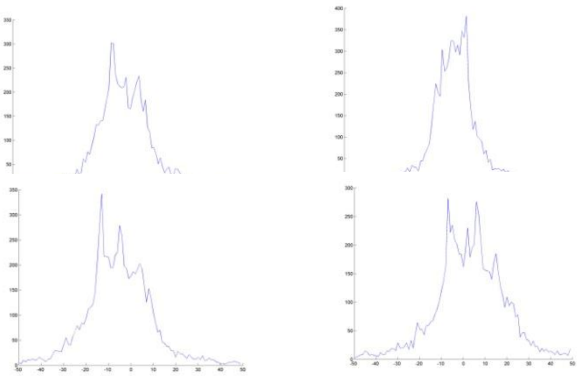

Fig. 23 The distributions of real values of the convergent sets for *a = 0.2*, *θ=(75*π/180)* and *degree = 3* in the codomain.

5.2 Hierarchical Structures

The convergent sets in Fig. 22 have more internal structures as we examine in details. In the following, we study another set of parameters in equation (9) as below:

$a = 0.1\ (\cos(120*\pi/180) + \sin\ (120*\pi/180)\ )$ with $degree = 3$ (9)

The convergent sets in codomain as shown in Fig. 24(a) are further expanded in Fig. 24(b).

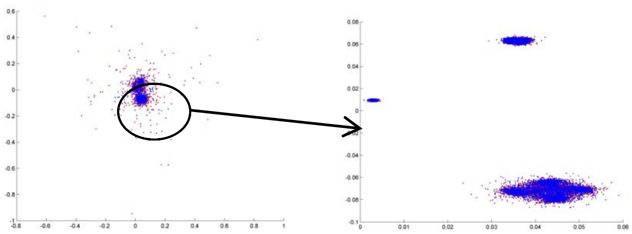

(a) Convergent sets in codomain (b) Expanded the circled area in (a)

Fig. 24. The distributions of the convergent sets for $a = 0.1$, $\theta=(120*\pi/180)$ and $degree = 3$ in the codomain.

We further expand the plot the three convergent groups of Fig. 24(b) to three individual plots as shown in Fig. 25. Then we select one of four sub-groups in Group 1 as shown Fig. 25(a), and expand one more level (2nd level) down to show the convergent sets as in Fig. 26.

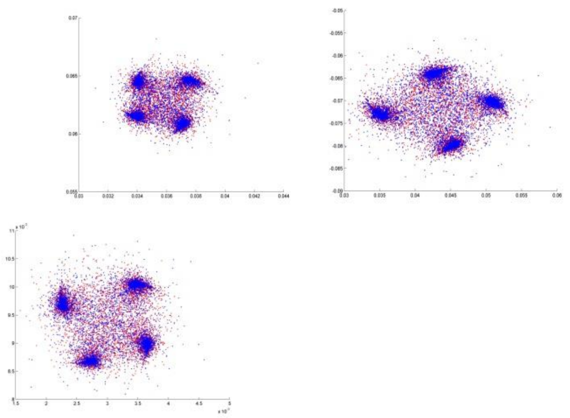

(a) Group 1 (b) Group 2 (c) Group 3

Fig. 25. The 1st-level expanded distributions of the convergent sets for $a = 0.1$, $\theta=(120*\pi/180)$ and $degree = 3$ in the codomain.

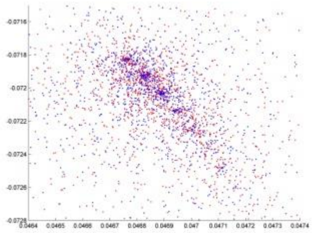

Fig. 26. The 2nd -level expanded distributions of the convergent sets for $a = 0.1$, $\theta=(120*\pi/180)$ and *degree* = *3* in the codomain.

Fig. 25 and 26 show that there are different stable sets on the complex plane. These results are adopted hereby to interpret the observed phenomena related to dark energy. Using Fig. 26 as an example, we can read that the individual set is with higher angular momentums and lower linear momentums and vice versa. While other stable individual set is with higher angular momentums and higher linear momentums.

Quaternion Mapping

On complex plane, however, spin momentum is limited to a single and discrete value for performing functional mapping, therefore, we extend to quaternion maps for further exploring the chaotic transitions as well as for potentially modelling Standard model of elementary particles with set structures forming group representations [8], which are the framework of quantum formalism for theorizing family structure of elementary particles.

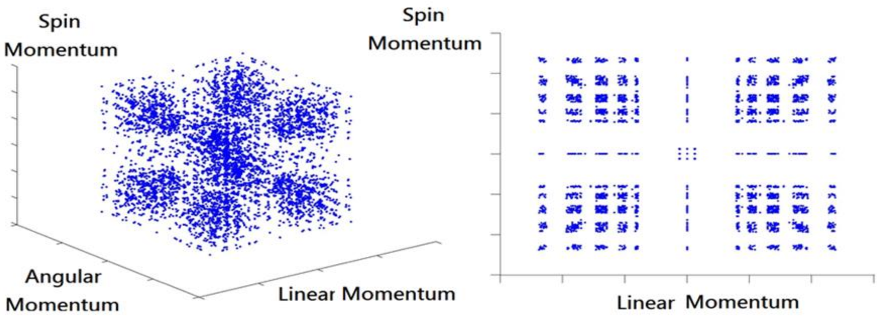

Fig. 27. 3D (Left) and 2D (Right) views of Quaternion Cubic

Fig. 27 shows 3D (linear-angular-spin) and 2D (linear-spin) views of quaternion mapping. Quaternion multiplication: $i^2 = j^2 = k^2 = ijk = -1$ is performed directly with EBF mapping. Fig. 28 shows the 2D views of quaternion mapping for *degree=1* through *degree = 5* with value of linear momentum $\{a\}$ equal to *0.1*.

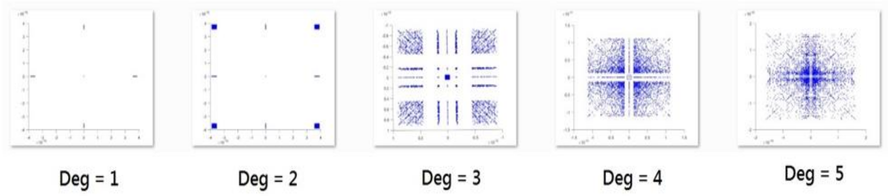

Fig. 28. 2D (Right) views of Quaternion Cubic

To propose the set structure for group representation of standard model, in this case, we select *degree = 3* since other set structures are not sufficient to support standard model. Further studies are undertaken to explore this effort. For comparing quaternion mapping with complex mapping, we can compare transitions, chaos, as well as formation of hierarchical structures. Fig. 29 shows linearization of quaternion mapping as value of linear momentum, $\{a\}$, approaching to unity [12].

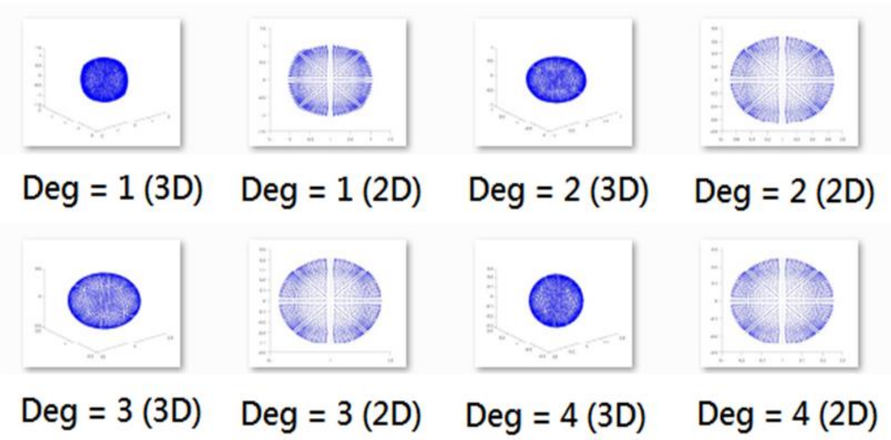

Fig. 29. Linearization of quaternion mapping as value $\{a\} = 0.99$

Remarks

In this paper, we perform complex and quaternion mapping in domain and codomain of extended Blaschke product (EBP) in conjunction with linear-angular-spin momentum triplet. This framework is proposed to model challenging physical phenomena, such as dark matters, dark energy, formation of stellar systems, quantum uncertainty, phase and superconductor transitions etc., particularly when the structures evolving from stable forms to chaos, where we have observed formation of hierarchical systems.

Further extension from complex mapping to quaternion mapping, we observe set structures, which potentially construct group presentations for standard model of elementary particles. This effort is undertaken with dark matter modelling.

We can summarize our studies as follows:

- Complex mapping of EBF with linear-angular-spin momentum triplet demonstrates structure richness for modelling physical phenomena.
- The pre-chaos hierarchical convergent sets in domain and codomain potentially provide models for formation and structure of galaxy clusters and stellar systems, and further for modelling dark matters and dark energies.
- Quaternion mapping of EBF with momentum triplet demonstrates set structures in codomain for constructing group representations for Beyond-Standard-Model efforts
- This constructed framework is potentially for grand unification theories (GUT).

References

[1] W. Blaschke, Eine Erweiterung des Satzes von Vitali, *über Folgen analytischer Funktionen*, Berichte Math.-Phys. Kl., Sächs. Gesell. der Wiss. Leipzig , No. 67, pp. 194–200, 1915.

[2] D. C. Ni and C. H. Chin, *$Z^{-1}C_1C_2C_3C_4$ System and Application,* Proceedings of TIENCS workshop, Singapore, August 1-5, 2006.

[3] D. C. Ni and C. H. Chin, *Symmetry Broken in Low Dimensional N-body Chaos*, Proc. of Chaos 2009 Conference, Chania, Crete, Greece, pp. 53 (Abstract), June 1-5, 2009.

[4] D. C. Ni and C. H. Chin, *Symmetry Broken in low dimensional N-Body Chaos*, CHAOTIC SYSTEMS: Theory and Applications (ed. by C. H. Skisdas and I. Domotikalis), pp. 215-223, 2010

[5] D. C. Ni, *Chaotic Behaviour Related to Potential Energy and Velocity in N-Body Systems,* Proceedings of 8th AIMS International Conference on Dynamical Systems, Differential Equations and Applications, May 25-28, 2010, Dresden, Germany, pp. 328.

[6] D. C. Ni and C. H. Chin, *Classification on Herman Rings of Extended Blaschke Equations*, Differential Equations and Control processes, Issue No. 2, Article 1, 2010.

[7] D. C. Ni, *Numerical Studies of Lorentz Transformation*, Proceeding of 7th EASIAM, Kitakyushu, Japan, June 27-29, 2011, pp. 113-114.

[8] C. Furey, “Generations: Three Prints, in Colour”, JHEP, 10, pp. 46-50

[9] D. C. Ni, *Statistics constructed from N-body systems*, Proceeding of World Congress, Statistics and Probability, Istanbul, Turkey, July 9-14, 2012, pp. 171.

[10] D. C. Ni, *Phase Transition Models based on A N-Body Complex Statistics*, Proceedings of the World Congress on Engineering 2013 (WCE 2013), Vol I, pp. 319-323, London, UK, July 3 - 5, 2013.
[11] D. C. Ni, *A Counter Example of Fundamental Theorem of Algebra: ExtendedBlaschke Mapping*, Proceedings of ICM 2014, August 13-August 21, Seoul, Korea, 2014.
[12] D. C. Ni, *Chaos in Complex and Quaternion Blaschke Maps*, Chaos 2018, June 5 – 8, Rome, Italy.